Effect of Terminal Group Modification on the Solution Properties of Dendrimers: A Molecular Dynamics Simulation Study

Nicholas W. Suek and Monica H. Lamm*

Department of Chemical and Biological Engineering, Iowa State University, Ames, Iowa 50011

Received January 24, 2006; Revised Manuscript Received April 10, 2006

ABSTRACT: We study the static and dynamic properties of amphiphilic dendrimers of generation 3 through 7 in an explicitly modeled solvent with molecular dynamics. All interior monomers are solvophobic while the terminal monomers are varied from all solvophobic to all solvophilic, with a number of nonuniform solvophobic/solvophilic terminal monomer arrangements investigated. For generations 6 and 7, crowding at the dendrimer surface forces some solvophilic monomers into the interior of the molecule. The nonuniformly surface-modified dendrimers are studied to examine how different arrangements of terminal monomers might affect dendrimer conformation. In all cases with solvophilic terminal monomers we find the solvophilic monomers congregating at the surface; thus, the dendrimer adopts the form of a unimolecular micelle. For generation 5 and smaller, the terminal monomer arrangement has no effect on the static or dynamic properties. For generations 6 and 7, a minimum number of bonds between the two types of terminal monomers is required to observe all solvophilic terminal monomers at the surface of the molecule. Lowering the simulation temperature, which effectively increases the interaction strength between solvophilic monomers and solvent, eliminates the backfolding tendencies of the solvophilic monomers and increases the asphericity of the generation 6 and 7 dendrimers.

1. Introduction

Dendrimers are synthetic macromolecules with regular and highly branched architectures. They are synthesized with a series of controlled reactions, where each step (generation) results in an exponential increase in the number of monomers. Because of their structural precision, they can be considered a synthetic analogue to proteins,[1,2] and there is interest in developing applications in medicine,[3−8] surface science,[9−12] and catalysis.[13−15] By modifying the chemical nature of the large number of terminal groups present in the dendrimer, one can alter properties, such as solubility[16] and toxicity.[3] The intent of this paper is to investigate the structure and mobility of monomers in amphiphilic dendrimers. Inspired by nonuniformly surface-modified dendrimers[17−19] (where there are more than one type of chemical functionality at terminal ends) synthesized with the convergent approach,[20,21] we use molecular simulation to explore static and dynamic conformational properties for a range of dendrimers with different surface-modified topologies.

Several workers have used Monte Carlo,[22] molecular dynamics,[23] and Langevin dynamics[24] simulations to study the structure and scaling properties of homo-dendrimers in solution; highlights from these studies are discussed in a recent review.[25] Murat and Grest[24] used Langevin dynamics to perform the first computational study examining the effects of solvent quality on a single, flexible homo-dendrimer in solution. They demonstrated that the monomer density decreases moving radially away from the dendrimer core and that terminal monomers are located at all distances from the core. This so-called "backfolding" phenomenon has since been confirmed experimentally.[26−28] Because the solvent is modeled implicitly through a white noise term in Langevin dynamics, Karatasos et al.[23] conducted molecular dynamics simulations of a homo-dendrimer in explicit solvent. These authors also observed backfolding in dendrimers at the theta condition, where interactions between the monomers and solvent are equally favorable.

* Corresponding author. E-mail: mhlamm@iastate.edu.

Only a few molecular simulation studies have considered dendrimers composed of more than one type of monomer, where each monomer type interacts differently with the surrounding solvent, i.e., an amphiphilic dendrimer.[16] Connolly et al.[29] used Metropolis Monte Carlo to study amphiphilic dendrimers of generation 1−7, with varying spacer length (number of bonds between branch points) where the solvent was modeled implicitly by tuning the effective monomer−monomer interactions. Giupponi and Buzza[30] used lattice-based configurational-bias Monte Carlo to study amphiphilic dendrimers by altering the relative strengths of terminal monomer−solvent and interior monomer−solvent interactions. In both studies, the dendrimers formed micelle-like structures, with the monomers in poor solvent congregating in the dendrimer's interior, regardless of whether they were, topologically speaking, a terminal or interior monomer.

In this paper, we perform molecular dynamics simulations of amphiphilic dendrimers with different arrangements of terminal monomers in explicit solvent. Highlights of our results include the following. Amphiphilic dendrimers form micelle structures with the solvophilic monomers congregating at the surface. At higher generations, the appearance of solvophilic monomers at the surface was reduced due to surface crowding. The arrangement of terminal monomers in the nonuniformly surface-modified dendrimers only had an effect on the structure and monomer mobility of the higher generation dendrimers. Lowering the simulation temperature, which effectively increased the interaction strength between solvophilic monomers and solvent, reduced the backfolding of terminal monomers and increased the asphericity of the higher generation dendrimers.

The paper is organized as follows. Section 2 details our model and simulation technique. The static and dynamic properties and the effects of temperature are presented in section 3. A brief summary and further discussion are given in section 4.

2. Method

We simulated a single dendrimer in explicit solvent using molecular dynamics. The dendrimer model consists of bead−

10.1021/ma060177z CCC: $33.50
Published on Web 05/13/2006

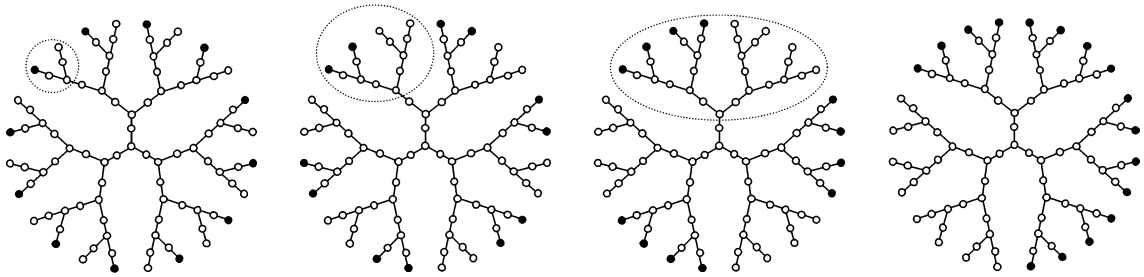

Figure 1. Four arrangements used for a nonuniform solvophobic/solvophilic exterior G3 dendrimer. The dendrimers are named, from left to right, G3-1_2, G3-2_4, G3-4_8, and G3-8_24 (see text for explanation). The white circles are solvophobic monomers, and the black are solvophilic monomers. In the symmetric arrangements, the dotted line outlines the fewest number of monomers needed to trace the number of bonds between solvophilic and solvophobic terminal monomers.

spring, freely jointed united-atom monomers. The solvent molecules are modeled as united-atom spheres. Molecular dynamics trajectories were generated by solving Newton's equations of motion, where the position, $\mathbf{r}_i(t)$, of the ith monomer or solvent particle with mass, m, is given by

$$m\frac{\mathrm{d}^2}{\mathrm{d}t^2}\mathbf{r}_i(t) = -\nabla\sum_j [U_{\mathrm{LJ}}(r_{ij}) + U_{\mathrm{bond}}(r_{ij})] \qquad (1)$$

where r_{ij} is the distance between monomers and/or solvent particles. Nonbonded interactions, U_{LJ}, are calculated with a truncated and shifted Lennard-Jones interaction potential[31]

$$U_{\mathrm{LJ}}(r_{ij}) = \begin{cases} 4\epsilon\left[\left(\frac{\sigma}{r_{ij}}\right)^{12} - \left(\frac{\sigma}{r_{ij}}\right)^{6} - \left(\frac{\sigma}{r_{cij}}\right)^{12} + \left(\frac{\sigma}{r_{cij}}\right)^{6}\right], & r_{ij} \le r_{cij} \\ 0, & r_{ij} > r_{cij} \end{cases} \qquad (2)$$

where ϵ is the well depth, σ is the particle diameter and r_{cij} is the cutoff radius. For all monomers and solvent particles, $\epsilon = 1$, $\sigma = 1$, and $m = 1$. Values selected for the cutoff radius will be discussed below. The bonded monomer interactions, U_{bond}, are calculated with a harmonic spring potential

$$U_{\mathrm{bond}}(r_{ij}) = K(r_{ij} - r_0)^2 \qquad (3)$$

where $K = 1662\epsilon/\sigma^2$ is the spring constant and $r_0 = \sigma$ is the equilibrium bond length.

The dendrimers in this study have N monomers (including the core), governed by the formula[32]

$$N = \frac{nb[(b-1)^{g+1} - 1]}{b-2} + 1 \qquad (4)$$

where g is the number of generations, b is the branch point functionality, and n is the number of bonds between branch points. In all simulations, $b = 3$ and $n = 2$. Figure 1 illustrates the dendrimer model for $g = 3$ (G3). There are two types of monomers in the simulation: (i) solvophilic, which have attractive and repulsive interactions with the solvent particles, and (ii) solvophobic, which have only repulsive interactions with the solvent particles. The interactions of solvophilic and solvophobic monomers with solvent particles are implemented by selecting cutoff radii of $r_{cij} = 2.5\sigma$ and $r_{cij} = 2^{1/6}\sigma$, respectively. All particles (solvophilic and solvophobic monomers, solvent) experience attractive interactions with their own type and thus have a cutoff radii of $r_{cij} = 2.5\sigma$. Solvophilic and solvophobic monomers have repulsive interactions and thus have cutoff radii of $r_{cij} = 2^{1/6}\sigma$. The cutoff radii for all particles are summarized in Table 1.

Table 1. Cutoff Radii for All Pairs of Monomers and Solvent Particles

particle i	particle j	r_{cij}
solvophobic monomer	solvophobic monomer	2.5σ
solvophobic monomer	solvophilic monomer	$2^{1/6}\sigma$
solvophobic monomer	solvent particle	$2^{1/6}\sigma$
solvophilic monomer	solvophilic monomer	2.5σ
solvophilic monomer	solvent particle	2.5σ
solvent particle	solvent particle	2.5σ

All monomers that are bonded to two or more monomers (core, branch point, and spacer) are considered interior monomers and are solvophobic. This is different from the two previous studies[29,30] in that they considered all monomers in the terminal generation to be terminal monomers. This difference results in roughly 50% of monomers in the previous studies being terminal while only 25% in the present study are terminal monomers. Terminal monomers are varied from all solvophobic to all solvophilic, depending on the arrangement being simulated. The uniformly solvophilic terminal monomer case is most similar to the "inner-H" case of ref 29 and the C1 and C2 cases of ref 30. Another difference between the three studies is that in the present study an interior monomer has the same attraction toward a terminal monomer or the solvent while in the two previous studies an interior monomer preferred to interact with a terminal monomer more than the solvent. We examined two nonuniform terminal monomer cases that could plausibly be constructed using a convergent synthesis method.[20] The first case consists of the different arrangements possible when half of the terminal monomers are solvophobic and the other half are solvophilic. Figure 1 shows the three possible combinations to achieve a symmetric half and half case for G3 dendrimers. There is a minimum of four bonds between solvophobic and solvophilic terminal monomers in a G3-1_2 dendrimer. There is a minimum of eight bonds between the two types of terminal monomers in a G3-2_4 dendrimer. The first number in the naming convention is the generation, the second is the number of solvophobic terminal monomers in the outlined area of Figure 1, and the third is the total number of terminal monomers in the outlined area. The second case consists of one of the three dendritic wedges attached to the core being terminated with all solvophobic monomers and the other two being terminated with all solvophilic monomers. These dendrimers are named G3-8_24 (shown in Figure 1), G4-16_48, G5-32_96, G6-64_192, and G7-128_384, where the second number is the number of solvophobic terminal monomers in the dendrimer and the third is the total number of terminal monomers.

The dendrimers were constructed with a series of self-avoiding random walks (step length $\approx r_0$) from the core monomer, following the algorithm used by Lescanec and Muthukumar,[33] until the desired generation was achieved. For G7, it was impossible to build dendrimers from the core without

Table 2. Number of Monomers and the Range of the Number of Solvent Particles in a Simulation of a Dendrimer of a Specific Generation

generation	monomers	solvent particles
3	91	2067−3467
4	187	4329−6530
5	379	6383−15362
6	763	13068−28087
7	1531	29153−34893

gross overlap of monomers. In these cases, we used a relaxed dendrimer of the previous generation as a starting point.[24] Solvent particles were then randomly added to the simulation volume, avoiding gross overlaps of particles and monomers, until a number density of 0.6 particles and monomers per unit volume was achieved. Table 2 shows the number of monomers and the range of solvent particles that were simulated for a dendrimer of a specific generation. The side length of the cubic simulation region was chosen to be 5−6 times the relaxed radius of gyration of the dendrimer, so that the dendrimer would not interact with periodic images of itself. To be certain that the results would not be affected by this choice of box size, a uniformly solvophilic terminated G3 dendrimer was simulated in larger periodic boxes.[23] There was no evidence of size effects on the static (structure factor) or dynamic (mean-square displacement and autocorrelation functions) properties of the dendrimer.

The simulations were carried out using LAMMPS 2004,[34,35] with a time step of $\Delta t = 0.0012\tau$, where $\tau = \sigma\sqrt{m/\epsilon}$. The initial configuration was relaxed for 2 million time steps at the desired temperature using the Nosé−Hoover thermostat.[31] The simulation temperatures chosen were $k_BT/\epsilon[=]T^* = 3.33$, 1.5, and 0.67, where k_B is the Boltzmann constant. For some cases, the run was repeated with a relaxation period of 500 000 time steps at $T^* > 6.5$, where the dendrimer has a more extended conformation, before relaxing the dendrimer further for 1.5 million time steps at $T^* = 3.33$. In both cases the equilibrium properties of the dendrimer were very similar. The thermostat was then turned off, and the production portion of the simulation was run for 10 million time steps at constant energy, so that the dynamic properties would be independent of the thermostat. The longest relaxation time can be estimated as $\tau_r = R_g^2/(6D)$, where D is the diffusion coefficient and R_g is the radius of gyration. This is the time required for the dendrimer to move a distance equal to its own size.[36] All G7 dendrimers, the largest and slowest moving of the dendrimers simulated, had $\tau_r \leq 1000\tau$. Thus, snapshots of the monomers' positions were saved every 1000 time steps to evaluate properties. The length of the production portion of the simulation was 12000τ. The uniform solvophilic terminal monomer cases for G3 and G6 as well as the uniform solvophobic terminal monomer case for G3 were repeated for two additional initial configurations, so that averages and standard deviations could be reported.

3. Results and Discussion

In this section we discuss the results of the simulation runs. All distances are reported in units of σ and times in units of τ. The radius of gyration, density profile, and shape analysis for $T^* = 3.33$ will be discussed in the first subsection. The second subsection will discuss the dynamic properties of mean-square displacement and autocorrelation functions for $T^* = 3.33$. The final subsection will examine the effect of temperature on the static properties of dendrimers with uniform solvophilic terminal monomers.

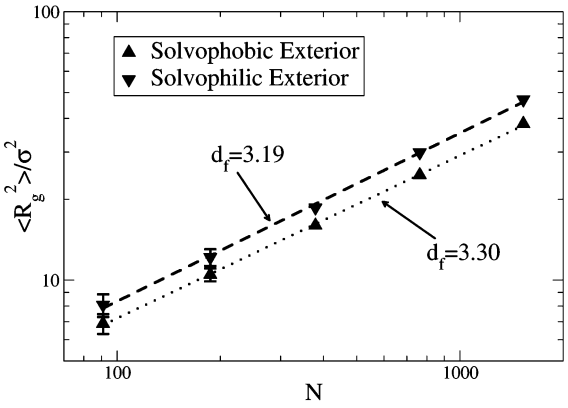

Figure 2. Average mean-square radius of gyration vs the number of monomers in the dendrimer. Average of 10 000 snapshots taken every 1000 time steps. Error bars are one standard deviation of the mean and are shown when larger than the symbol size. The dashed (solvophilic terminal monomers) and dotted (solvophobic terminal monomers) lines are linear fits used to determine the fractal dimension.

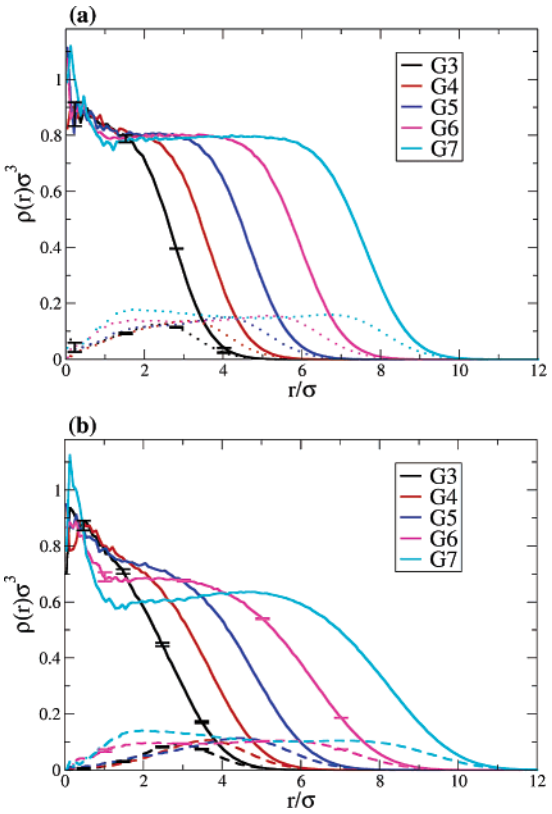

Figure 3. Radial monomer densities for different generations of dendrimers with uniform terminal monomers: (a) solvophobic and (b) solvophilic. The solid lines are the density of all monomers in each dendrimer. The dotted and dashed lines are the density of solvophobic and solvophilic, respectively, terminal monomers and are color-coded to the corresponding total density line. The data shown are the average of 10 000 snapshots taken every 1000 time steps. The error bars, of four arbitrarily chosen points, are one standard deviation of the mean.

3.1. Static Properties. A measure of the overall size of a dendrimer is the radius of gyration

$$\langle R_g^2 \rangle = \frac{1}{N}\sum_i^N |\mathbf{r}_i - \mathbf{R}|^2 \quad (5)$$

where **R** is the center of mass. Radii of gyration are shown in Figure 2 for dendrimers with terminal monomers that are either entirely solvophobic or solvophilic. The radius of gyration scales

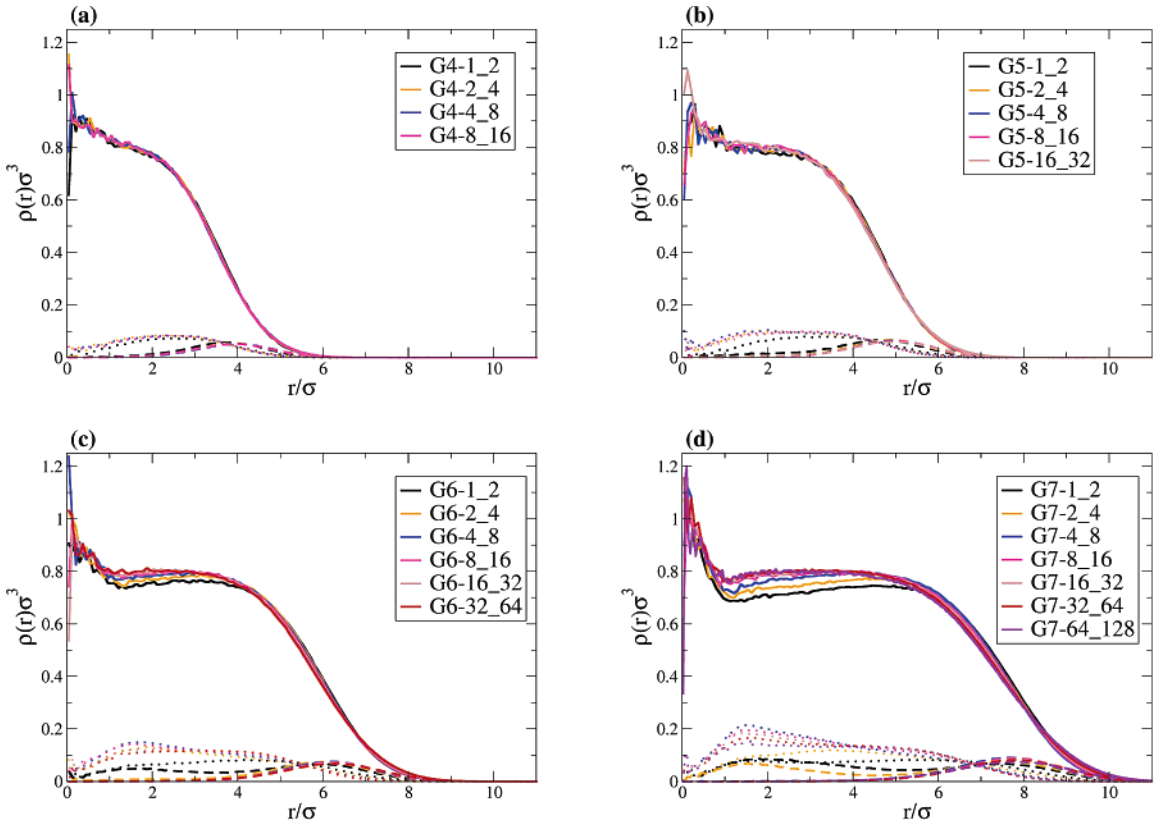

Figure 4. Radial monomer densities for different generations of dendrimers with nonuniform (50% solvophobic and 50% solvophilic) terminal monomers: (a) G4, (b) G5, (c) G6, and (d) G7. Symbols and averaging as in Figure 3.

with N, as $R_g^2 \propto N^{2/d_f}$, where d_f is the fractal dimension.[37] The fractal dimensions for dendrimers with solvophilic and solvophobic terminal monomers are 3.19 ± 0.07 and 3.30 ± 0.03, respectively. Although these fractal dimensions are greater than the dimensionality of Euclidean space, these results roughly describe the $R_g \propto N^{1/3}$ scaling behavior seen for dendrimers in poor solvents by previous studies.[38,39]

The radial monomer density profile, $\rho(r)$, shows the number of monomers within a spherical shell of radius, r, and thickness, 0.083σ, from the dendrimer center of mass per volume of the shell. Radial monomer density profiles will be displayed for all monomers and for each type of terminal monomer. Figure 3 shows the density profiles for dendrimers with uniform terminal monomers. The solvophobic exterior case demonstrates that the core is the most dense region of the dendrimer and the density decreases as the exterior is approached. The profiles also demonstrate backfolding, as terminal monomers are located at all distances from the center of mass. As dendrimer generation increases, the probability of finding a terminal monomer near the center of mass also increases. For all generations, the total monomer density between the center of mass and the surface plateaus at the same density. The plateau has greater density than the total system density and is a result of a deficit of material immediately surrounding the dendrimer that reduces unfavorable interaction of solvophobic monomers and solvent.

The solvophilic exterior case shows that for generations less than six the solvophilic terminal monomers are drawn away from the center and toward the solvent outside the molecule. For G6 and greater the solvophilic terminal monomers are located throughout the molecule, presumably forced back by overcrowding at the surface due to the fact that as generation increases the number of terminal monomers increases exponentially while the available surface area only increases as a

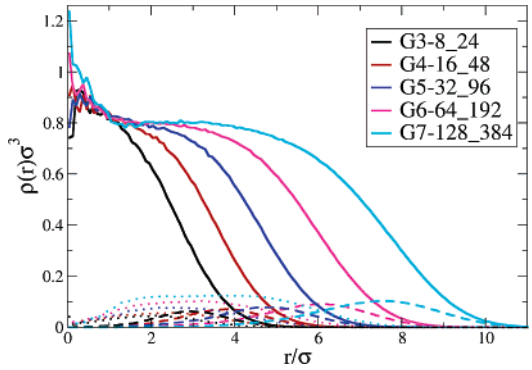

Figure 5. Radial monomer densities for different generations of dendritic wedge dendrimers. Symbols and averaging as in Figure 3.

square. The total monomer density plateau that exists for the completely solvophobic case disappears, except for G6 where the profile shifts from monotonically decreasing (for lower generations) to profiles with a minimum between the center of mass and the surface. This minimum allows for the presence of solvent inside the dendrimer. Inside the dendrimer, solvent particles have a radial density (not shown) that is slightly less than the density of solvophilic monomers.

It is possible that the generation at which solvophilic terminal monomers are forced inward depends on the system density. For example, in a system of higher density, the generation at which solvophilic terminal monomers distribute throughout the dendrimer interior might be smaller than that for a system of lower density. To determine whether the presence of solvophilic terminal monomers near the core for a given generation is dependent on system density, a solvophilic exterior G6 dendrimer was simulated with a system of number density 0.3. The density profile was similar to the profile for the system with

Table 3. Asphericity of Dendrimers with Configuration and Generation[a]

arrangement	G3	G4	G5	G6	G7
solvophobic	0.082 (0.018)	0.052 (0.008)	0.032 (0.003)	0.022 (0.001)	0.012 (0.0004)
solvophilic	0.096 (0.026)	0.063 (0.012)	0.052 (0.007)	0.048 (0.005)	0.022 (0.002)
"one-third"	0.094 (0.025)	0.059 (0.010)	0.049 (0.006)	0.034 (0.003)	0.023 (0.001)
1_2	0.087 (0.020)	0.057 (0.010)	0.038 (0.004)	0.030 (0.002)	0.018 (0.001)
2_4	0.086 (0.021)	0.051 (0.008)	0.035 (0.004)	0.030 (0.002)	0.022 (0.001)
4_8	0.091 (0.022)	0.055 (0.009)	0.034 (0.003)	0.025 (0.002)	0.017 (0.001)
8_16		0.060 (0.010)	0.032 (0.003)	0.022 (0.001)	0.013 (0.001)
16_32			0.042 (0.005)	0.024 (0.002)	0.015 (0.001)
32_64				0.031 (0.002)	0.014 (0.001)
64_128					0.029 (0.002)

[a] Results are averages over 10 000 snapshots taken every 1000 time steps. One standard deviation from the mean is inside parentheses. Solvophobic and solvophilic refer to uniform terminal monomer cases. "One-third" refers to whole dendritic wedge configuration with one-third of terminal atoms being solvophobic.

number density 0.6, with terminal monomers appearing near the center of mass. A solvophilic exterior, G5 dendrimer was simulated in a system with number density 0.9, and the density profile was similar to the profile with number density 0.6, with no terminal monomers appearing near the center of mass.

Now we examine the case where dendrimers have nonuniform terminal monomers consisting of half solvophobic and half solvophilic terminal monomers. Figure 4 shows density profiles for dendrimers G4 to G7 with nonuniform terminal monomers. The arrangement of solvophilic and solvophobic terminal monomers does not affect the density profile of nonuniform terminal monomer dendrimers for generations less than six. At higher generations, crowding at the surface influences the arrangement of the terminal monomers. For G6-1_2, G7-1_2, and G7-2_4, solvophilic terminal monomers are found near the center of mass, whereas for the other G6 and G7 terminal group configurations the solvophilic monomers remain at the surface. This can be explained by noting the minimum number of bonds between solvophilic and solvophobic terminal monomers for a given arrangement. To relieve overcrowding at the periphery, portions of the dendrimer must backfold into the interior. For terminal monomer arrangements with a low repeat pattern, this means that some solvophilic monomers will be taken into the dendrimer's interior because there are not enough bonds separating the opposing monomers to allow them to segregate. As the repeat pattern increases, larger and larger portions of the dendrimer are free to segregate, thereby allowing the solvophilic terminal monomers to remain at the surface while the solvophobic terminal monomers backfold into the interior.

Next we consider nonuniform terminal monomer dendrimers built by keeping the terminal monomers on each of the three dendritic wedges attached to the core the same so that two-thirds of the terminal monomers are solvophilic and the remaining third are solvophobic. Figure 5 shows the density profiles for these dendrimers. There is sufficient room at the surface of the dendrimer up to G7 for all solvophilic monomers to appear near the surface.

The density profiles shown may be misleading if the molecule is adopting an oblong shape where a uniform distance from the center of mass does not represent the "surface". To test for this possibility, we characterized the shape of the dendrimer by calculating the asphericity[40,41]

$$\delta = 1 - 3\langle I_2\rangle/\langle I_1^2\rangle \tag{6}$$

where I_1 and I_2 are the first two invariants

$$I_1 = \lambda_1 + \lambda_2 + \lambda_3 \tag{7}$$

$$I_2 = \lambda_1\lambda_2 + \lambda_2\lambda_3 + \lambda_1\lambda_3 \tag{8}$$

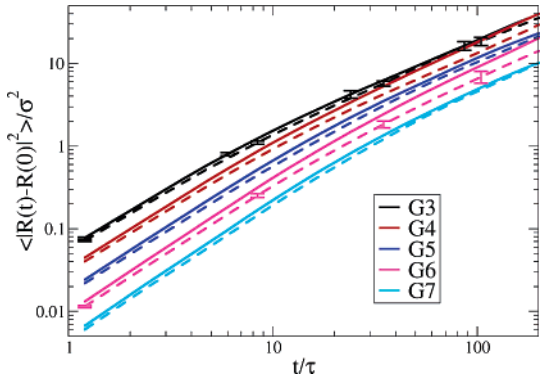

Figure 6. Mean-square displacement of the center of mass for different generations of dendrimers with uniform terminal monomers. The solid line is the mean-square displacement of the uniform solvophobic terminal monomer dendrimer, and the dashed line is that of the uniform solvophilic terminal monomer dendrimer. The error bars, of four arbitrarily chosen points, are one standard deviation of the mean.

and λ_1, λ_2, and λ_3 are the eigenvalues of the gyration tensor

$$G_{uv} = \frac{1}{N}\sum_i^N (r_{ui} - R_u)(r_{vi} - R_v) \tag{9}$$

where u and $v = x$, y, and z. The asphericity parameter can take values ranging from zero (sphere) to one (line). Table 3 shows that as the dendrimer generation increases, the asphericity decreases. The uniform solvophilic terminal monomer cases are more aspherical than their solvophobic analogues, and all nonuniform terminal monomer cases are between the two nonuniform cases, except for G7. In the 50/50 cases we see a minimum asphericity in the middle of the range of the minimum number of bonds between different terminal monomer types. All asphericity values are less than 0.1 (corresponding to one moment being 2.4 times larger than the other two or two moments being 3.6 times larger than the third, which are the extrema for all possible combinations of moments that have an asphericity of 0.1), implying the dendrimer does not take conformations that deviate a large amount from a spherical shape for all generations and configurations. Thus, radial density profiles are appropriate for determining the location of terminal monomers in these systems.

3.2. Dynamic Properties. We next examine the dynamic properties of the dendrimer. The translational diffusion coefficient, D, of the dendrimer can be determined by[31]

$$D = \lim_{t\to\infty} \frac{\langle|\mathbf{R}(t) - \mathbf{R}(0)|^2\rangle}{6t} \tag{10}$$

where the bracketed term is the center-of-mass mean-square

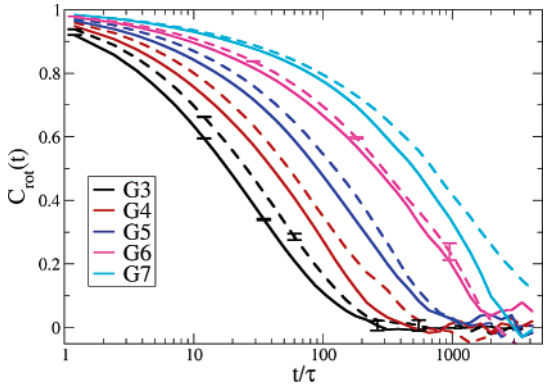

Figure 7. Rotational autocorrelation function for different generations of dendrimers with uniform terminal monomers. Symbols as in Figure 6.

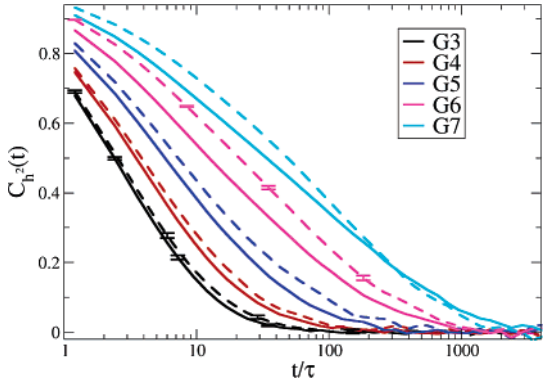

Figure 8. Terminal monomer pulsation autocorrelation function for different generations of dendrimers with uniform terminal monomers. Symbols as in Figure 6.

displacement. The dendrimer's center-of-mass mean-square displacement as a function of generation is given in Figure 6. It shows that the dendrimer's mobility decreases as its generation (mass) increases. It also indicates that as one goes from uniform solvophobic terminal monomers to the solvophilic analogue, which increases the radius of gyration, the mobility is decreased despite its increased attraction/affinity for the solvent. Therefore, it appears that linear/volumetric size is the driving force for mobility.

The rotational autocorrelation function

$$C_{\mathrm{rot}}(t) = \langle \mathbf{e}_i(0) \cdot \mathbf{e}_i(t) \rangle \tag{11}$$

of the molecule describes how fast the molecule is rotating and is best described by how a unit vector, $\mathbf{e}_i$, from the center of mass to a point on the surface is changing. Since the terminal monomer density profiles show that terminal monomers are most likely of all monomers to be at the surface, $\mathbf{e}_i$ is defined as the unit vector from the center of mass to a terminal monomer. Figure 7 shows the rotational autocorrelation function for dendrimers with uniform solvophobic and solvophilic terminal monomers. It agrees with previous studies[23,42] that show the relaxation is slower as the generation increases. It also shows solvophobic dendrimers relaxing faster than solvophilic, since the radii of gyration of dendrimers with solvophilic exteriors are larger so slower relaxation is not surprising.

The mobility of the terminal monomers is an important property to consider for applications where dendrimers are functionalized with ligands so that they may target and interact with cells and other biological species. The pulsations of terminal monomers can be measured by the autocorrelation

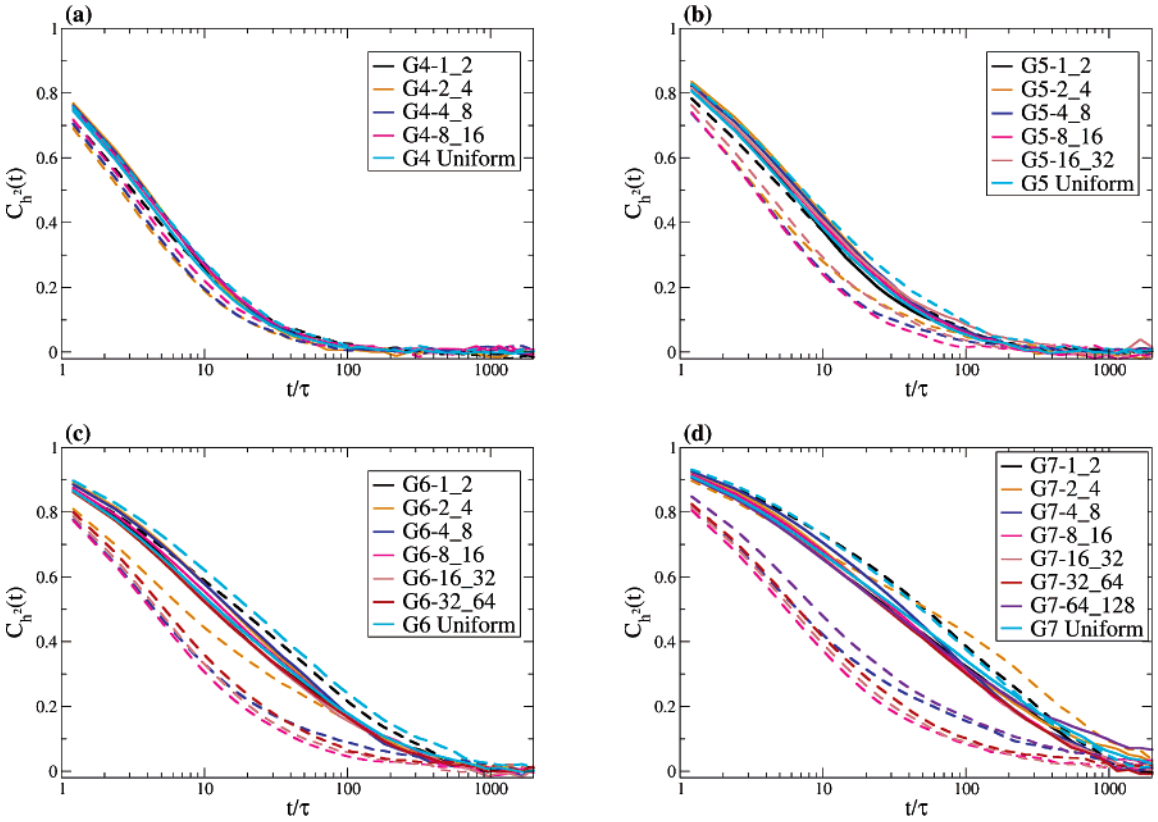

Figure 9. Terminal monomer pulsation autocorrelation function (ACF) for different generations of dendrimers with nonuniform terminal monomers: (a) G4, (b) G5, (c) G6, and (d) G7. The solid line is the ACF of the solvophobic terminal monomers, and the dashed line is that of the solvophilic terminal monomers. The cyan lines represent the ACF of dendrimers with uniform terminal monomers for that generation.

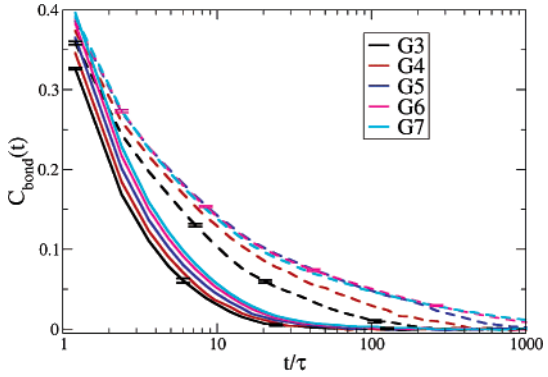

Figure 10. Terminal bond unit vector autocorrelation function for different generations of dendrimers with uniform terminal monomers. Symbols as in Figure 6.

function of the terminal monomer to center-of-mass distance

$$C_{h_{Tx}^2}(t) = \frac{1}{N_{Tx}} \sum_{i}^{N_{Tx}} \frac{\langle h_i^2(0)\, h_i^2(t)\rangle - \langle h_i^2\rangle^2}{\langle h_i^4\rangle - \langle h_i^2\rangle^2} \qquad (12)$$

where the subscript "Tx" refers to the type of terminal monomer and h_i is the distance between the center of mass and the ith terminal monomer. Figure 8 shows the pulsation autocorrelation function for dendrimers with uniform solvophobic and solvophilic terminal monomers. The mobility of terminal monomers decreases as the generation increases. The relative mobility of solvophobic to solvophilic terminal monomers increases with increasing generation until G6. At G7 the autocorrelation functions crossover each other before they have relaxed below the threshold of $C_{h_{Tx}^2} = 0.2$.

Figure 9 shows the pulsation autocorrelation function for dendrimers with patterned terminal monomer arrangements. Here we see the solvophobic terminal monomer retains a fairly constant mobility for a given generation. As the repeat pattern increases, thereby increasing the number of bonds between solvophilic and solvophobic terminal monomers, the mobility of the solvophilic monomer increases. The mobility of solvophilic monomers drops off somewhat at the maximum repeat pattern. We see that in the G6-1_2, G7-1_2, and G7-2_4 cases, where solvophilic terminal monomers are found in the interior, they are less mobile than the solvophobic terminal monomers. Overall, the solvophobic/solvophilic arrangement of terminal monomers has less effect on mobility for small generations than it does for large generations.

The orientational mobility of the terminal bond can be measured with the autocorrelation function of the unit vector from the terminal monomer to its bonded monomer

$$C_{bond}(t) = \langle \mathbf{b}_i(0)\cdot\mathbf{b}_i(t)\rangle \qquad (13)$$

Figure 10 shows the terminal bond autocorrelation function. The bond reorientates itself more freely with the solvophobic terminal monomer than with the solvophilic terminal monomer. Figure 11 shows the terminal bond autocorrelation function for dendrimers with patterned terminal monomer arrangements. Here we see the solvophobic terminal bond's mobility is independent of its proximity to solvophilic bonds. Among the cases with solvophilic terminal monomers, the relaxation of the solvophilic terminal bond is always fastest for the dendrimer with uniform solvophilic terminal monomers. This is in contrast to the trend observed for solvophilic terminal monomer pulsations in Figure 9.

3.3. Temperature Effects. In this section we examine the effects of temperature by comparing dendrimers with uniform solvophilic terminal monomers that were relaxed at reduced temperatures of 3.33, 1.5, and 0.67. Figure 12 shows the radius

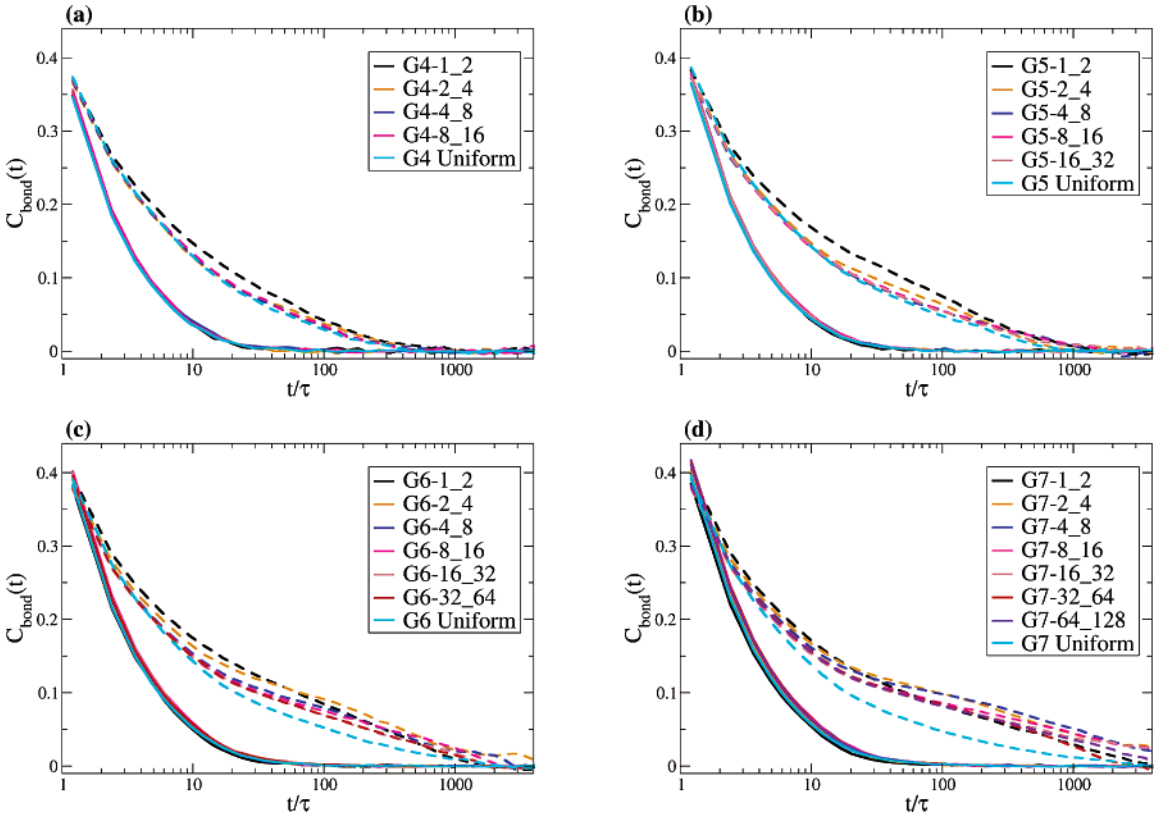

Figure 11. Terminal bond unit vector autocorrelation function for different generations of dendrimers with nonuniform terminal monomers: (a) G4, (b) G5, (c) G6, and (d) G7. Symbols as in Figure 9.

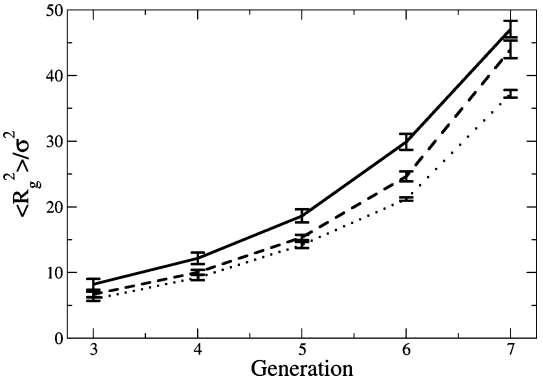

Figure 12. Radius of gyration vs generation for dendrimers with uniform solvophilic terminal monomers. The solid, dashed, and dotted lines are $T^* = 3.33$, 1.5, and 0.67, respectively. The error bars are one standard deviation of the mean. The lines are shown to guide the eye.

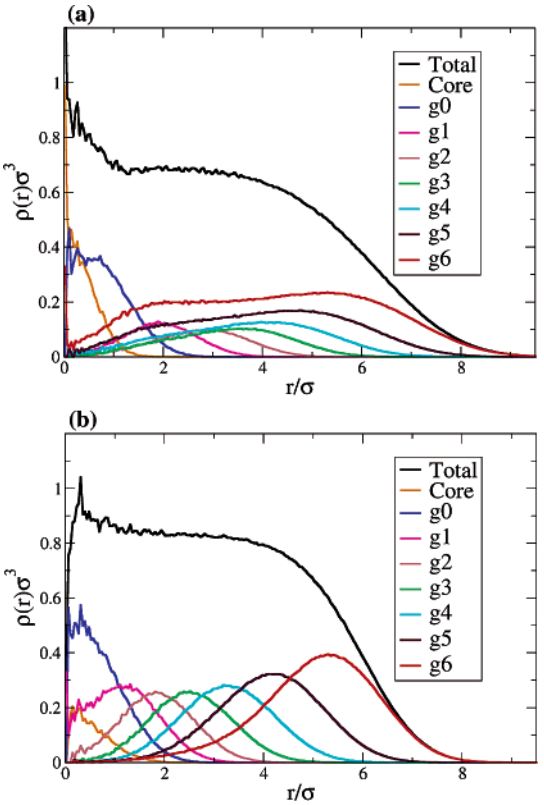

Figure 13. Radial monomer density profile resolved into generations for G6 at reduced temperatures: (a) 3.33 and (b) 1.5. Each line shows the density of monomers from one generation of the dendrimer in addition to the core monomer and a total monomer density. The data shown are the average of 10 000 snapshots taken every 1000 time steps.

of gyration vs generation for different temperatures. The radial monomer density profiles resolved into generations for G6 at reduced temperatures of 3.33 and 1.5 are shown in Figure 13. As the temperature decreases, the radius of gyration decreases and the monomer density plateau level increases, indicating the dendrimer is more compact. As the temperature decreases, the core monomer is more likely to be further away from the center of mass and there is less backfolding of monomers toward the center of mass. Figure 14 shows the asphericity vs generation for different temperatures. At $T^* = 0.67$, there is a local minimum at G6. Here energy dominates entropy, so all of the solvophilic monomers have congregated with the terminal bonds pointed away from the center of mass and as generation increases the surface coverage of solvophilic monomers increases until G6. At G7 the dendrimer was forced to adopt a

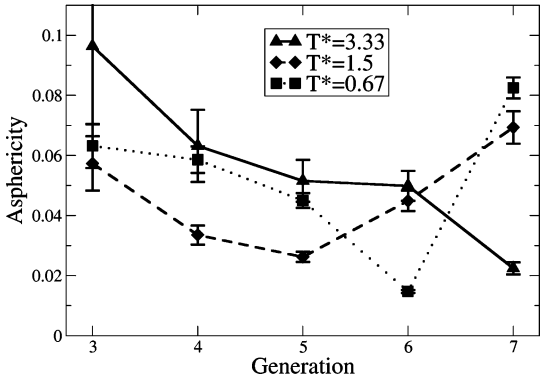

Figure 14. Asphericity vs generation for dendrimers with uniform solvophilic terminal monomers. Symbols as in Figure 12.

more aspherical conformation to increase the surface area. At $T^* = 3.33$, the asphericity decreases monotonically with increasing generation because the entropy has more influence over shape than the energy so that as more monomers are added (generation increases) the average conformation is more spherical, which maximizes the available volume, thereby increasing the number of possible conformations. Another possibility is that since raising the temperature in our system has the effect of decreasing the strength of attraction between pairs of monomers with attractive potentials, we have made our uniform solvophilic terminal monomer case more similar to the solvophobic analogue, where asphericity decreases monotonically with increasing generation. At $T^* = 1.5$, we see a minimum asphericity at G5. The finding of a minimum asphericity occurring between G4 and G6 (inclusive) in this study for $T^* \leq 1.5$ is similar to what was seen in the previous coarse-grained amphiphilic dendrimer studies[29,30] and an atomistic PAMAM dendrimer study.[43] An exception is that only ref 29 saw an elongation of the dendrimer, this despite the similarities between the models of refs 29 and 30, i.e., (i) a greater fraction of monomers are terminal monomers and (ii) the interior monomers prefer to interact with terminal monomers rather than the solvent. At G7 the asphericity increases with decreasing temperature and at G6 the asphericity decreases with decreasing temperature, although the asphericities for G6 at reduced temperatures 1.5 and 3.33 are within a standard deviation of each other. For G5 and below, the asphericity has minima at a reduced temperature of 1.5. This difference in trends may warrant additional study.

4. Conclusion

We used molecular dynamics to simulate amphiphilic dendrimers in explicit solvent. We found that amphiphilic dendrimers form micelle structures with the solvophilic monomers congregating at the surface. The ability of solvophilic monomers to congregate at the surface did not change below G6. At G6 and above, the uniform solvophilic terminal monomers were found throughout the dendrimer due to surface crowding. For the nonuniform terminal monomer G6 and G7 cases, if the number of bonds between the two types of terminal monomers was not large enough, a fraction of the solvophilic terminal monomers were found near the center of mass.

The global dynamics of the dendrimer slowed as the radius of gyration of the dendrimer increased, which was caused by either increasing generation or changing the terminal monomers from solvophobic to solvophilic. The local dynamics of the solvophilic terminal monomers was affected by the number of bonds between the two types of terminal monomers for G6 and G7. The local dynamics of the solvophobic terminal monomers did not change within generations for all generations.

As the simulation temperature was lowered, the uniform solvophilic terminal monomer dendrimers behaved less similar to the uniform solvophobic dendrimers with the G6 dendrimer avoiding the need for backfolding. The asphericity trends changed from monotonically decreasing (high temperature) to the presence of a minimum (lower temperatures).

Because of their ability to form unimolecular micelles, amphiphilic dendrimers can accomplish with one molecule what would require multiples of other molecules. This, coupled with the molecular "tuning" capability afforded by recent progress in dendrimer synthesis, makes dendrimers unique among macromolecules. In this paper, we have investigated how variations in terminal group chemistry impact the conformational and dynamic properties of dendrimers in solution. To our knowledge, this is the first study of its kind to explore the effects that nonuniform amphiphilic topologies have on dendrimer behavior.

Acknowledgment. This work was partially supported by an Iowa State University Special Research Initiation Grant (SPRIG). The computations were performed in part at the ISU High Performance Computing facility.

References and Notes

(1) Matthews, O. A.; Shipway, A. N.; Stoddart, J. F. *Prog. Polym. Sci.* **1998**, *23*, 1−56.
(2) DeMattei, C. R.; Huang, B.; Tomalia, D. A. *Nano Lett.* **2004**, *4*, 771−777.
(3) Boas, U.; Heegaard, P. M. H. *Chem. Soc. Rev.* **2004**, *33*, 43−63.
(4) Shaunak, S.; Thomas, S.; Gianasi, E.; Godwin, A.; Jones, E.; Teo, I.; Mireskandari, K.; Luthert, P.; Duncan, R.; Patterson, S.; Khaw, P.; Brocchini, S. *Nat. Biotechnol.* **2004**, *22*, 977−984.
(5) Fuchs, S.; Kapp, T.; Otto, H.; Schoneberg, T.; Frank, P.; Gust, R.; Schluter, A. D. *Chem.—Eur. J.* **2004**, *10*, 1167−1192.
(6) Khopade, A. J.; Caruso, F. *Biomacromolecules* **2002**, *3*, 1154−1162.
(7) Chauhan, A. S.; Jain, N. K.; Diwan, P. V.; Khopade, A. J. *J. Drug Target.* **2004**, *12*, 575−583.
(8) Aulenta, F.; Hayes, W.; Rannard, S. *Eur. Polym. J.* **2003**, *39*, 1741−1771.
(9) Tsukruk, V. V.; Rinderspacher, F.; Bliznyuk, V. N. *Langmuir* **1997**, *13*, 2171−2176.
(10) Tsukruk, V. V. *Adv. Mater.* **1998**, *10*, 253−257.
(11) Bosman, A. W.; Janssen, H. M.; Meijer, E. W. *Chem. Rev.* **1999**, *99*, 1665−1688.
(12) Emmrich, E.; Franzka, S.; Schmid, G. *Nano Lett.* **2002**, *2*, 1239−1242.
(13) Crooks, R. M.; Zhao, M.; Sun, L.; Chechik, V.; Yeung, L. K. *Acc. Chem. Res.* **2001**, *34*, 181−190.
(14) Crooks, R. M.; Lemon, B. I., III.; Sun, L.; Yeung, L. K.; Zhao, M. *Top. Curr. Chem.* **2001**, *212*, 81−135.
(15) Lang, H.; Luhmann, B. *Adv. Mater.* **2001**, *13*, 1523−1540.
(16) Krska, S.; Seyforth, D. *J. Am. Chem. Soc.* **1998**, *120*, 3604−3612.
(17) Hawker, C. J.; Frechet, J. M. J. *Macromolecules* **1990**, *23*, 4726−4729.
(18) Wooley, K. L.; Hawker, C. J.; Frechet, J. M. J. *J. Chem. Soc., Perkin Trans. 1* **1991**, 1059−1076.
(19) Wooley, K. L.; Hawker, C. J.; Frechet, J. M. J. *J. Am. Chem. Soc.* **1993**, *115*, 11496−11505.
(20) Hawker, C. J.; Frechet, J. M. J. *J. Am. Chem. Soc.* **1990**, *112*, 7638−7647.
(21) Frechet, J. M. J. *Science* **1994**, *263*, 1710−1715.
(22) Mansfield, M. L.; Klushin, L. I. *Macromolecules* **1993**, *26*, 4262−4268.
(23) Karatasos, K.; Adolf, D. B.; Davies, G. R. *J. Chem. Phys.* **2001**, *115*, 5310−5318.
(24) Murat, M.; Grest, G. S. *Macromolecules* **1996**, *29*, 1278−1285.
(25) Ballauff, M.; Likos, C. N. *Angew. Chem., Int. Ed.* **2004**, *43*, 2998−3020.
(26) Wooley, K. L.; Klug, C. A.; Tasaki, K.; Schaefer, J. *J. Am. Chem. Soc.* **1997**, *119*, 53−58.
(27) Ballauff, M. *Top. Curr. Chem.* **2001**, *212*, 177−194.
(28) Rosenfeldt, S.; Dingenouts, N.; Ballauff, M.; Werner, N.; Vogtle, F.; Linder, P. *Macromolecules* **2002**, *35*, 8098−8105.
(29) Connolly, R.; Timoshenko, E. G.; Kuznetsov, Y. A. *Macromolecules* **2004**, *37*, 7381−7392.
(30) Giupponi, G.; Buzza, D. M. A. *J. Chem. Phys.* **2005**, *122*, 194903.
(31) Frenkel, D.; Smit, B. *Understanding Molecular Simulation*, 2nd ed.; Academic Press: San Diego, CA, 2002.
(32) Tomalia, D. A.; Naylor, A. M.; Goddard, W. A. *Angew. Chem., Int. Ed.* **1990**, *29*, 138−175.
(33) Lescanec, R. L.; Muthukumar, M. *Macromolecules* **1990**, *23*, 2280−2288.
(34) Plimpton, S. *J. Comput. Phys.* **1995**, *117*, 1−19.
(35) http://www.cs.sandia.gov/sjplimp/lammps.html.
(36) Dunweg, B.; Kremer, K. *J. Chem. Phys.* **1993**, *99*, 6983−6996.
(37) Kaye, B. H. *A Random Walk Through Fractal Dimensions*, 1st ed.; VCH Publishers: Sudbury, 1989.
(38) Sheng, Y. J.; Jiang, S. Y.; Tsao, H. K. *Macromolecules* **2002**, *35*, 7865−7868.
(39) Giupponi, G.; Buzza, D. M. A. *J. Chem. Phys.* **2004**, *120*, 10290−10298.
(40) Rudnick, J.; Gaspari, G. *J. Phys. A* **1986**, *19*, L191−L193.
(41) Aronovitz, J.; Nelson, D. *J. Phys. (Paris)* **1986**, *47*, 1445−1456.
(42) Lyulin, S. V.; Darinskii, A. A.; Lyulin, A. V.; Michels, M. A. J. *Macromolecules* **2004**, *37*, 4676−4685.
(43) Maiti, P. K.; Cagin, T.; Wang, G. F.; Goddard, W. A. *Macromolecules* **2004**, *37*, 6236−6254.

MA060177Z